The Attitude Control System of the Delfi-N3xt Satellite

Jon Reijneveld
Chair of Space Systems Engineering
Delft University of Technology
J.P.J.Reijneveld@Student.TUDelft.NL

Daniel Choukroun
Chair of Space Systems Engineering
Delft University of Technology
D.Choukroun@TUDelft.NL

Extended Abstract

Following up with the successful mission of its first nano-satellite, Delfi-C^3, the Delft University of Technology (TUD) is currently undertaking the development of its next satellite, Delfi-n3Xt, which three major mission objectives are a single-point-of-failure free electrical power subsystem with energy storage, a high data rate link, and three-axis active attitude control. Similarly to Delfi-C^3, Delfi-n3Xt is a triple-unit CubeSat. Following the launch, foreseen as piggyback, the satellite will be deployed from a P-POD on a Sun synchronous orbit at an altitude yet to be selected within a $[600, 1000]$ km range. This work gives a partial account of the on-going developments of the Attitude Determination and Control Sub-system (ADCS), in particular, it presents the detumbling mode, the Sun pointing control modes (coarse and fine Sun acquisition), and the three-axis attitude control mode using perfect state information.

The ADCS is equipped with the following suite of sensors and actuators: a 3-axis magnetometer (MGM), a suite of coarse Sun sensors (CSS), a 3-axis MEMS rate gyro, three magnetorquers (MTQ), which are developed at TUD, and three reaction wheels (RW) which spinning mass is also designed at TUD. This suite of sensors and actuators provides redundancy in the ADCS. For the sake of fail-safe operations however, we consider the situation where the gyros and the reaction wheels are not operational. Much research has been conducted in the field of control strategies using magnetic information and actuation only (sample works in the realm of nano satellites are presented in Refs. [1, 2, 3, 4, 5, 6]). The widely adopted **b**-dot control [2] allows for the detumbling of the spacecraft dynamics following the separation phase. As a result, the satellite acquires a slow rotational motion, around the normal to its orbital plane, which rate is twice its orbital motion rate around the Earth. The **b**-dot law was further modified in order to produce a spin motion around a preferred body-axis [3, 1, 6]. The rationale for creating an additional spin motion stems from the resulting "gyroscopic rigidity" around the spin axis. It helps keeping a body axis along a preferred inertial axis, such as the line-of-sight (LOS) to the Sun along low Earth orbits (LEO) during eclipses, when the Sun sensors are not operational. The precession of the spin axis towards the Sun LOS can be achieved using Sun vector measurements and its time derivative, in conjunction with the Earth magnetic field measurements[1]. It also requires an estimate of the angular inertial angular velocity around the spin axis. The later information can be replaced by knowledge of the satellite angular momentum[6] but introduces a sensitivity to inertia uncertainties. In this work, building on Ref. [1], we adopt a three control modes strategy for the Sun acquisition and tracking algorithm and add a fourth control mode based a full state feedback control law derived in Ref. [4]. However, we suggest a modification of the Sun coarse acquisition law that alleviates the strong nonlinearity due to the absolute value. Extensive simulations have been performed to illustrate the performances of the control strategy with respect to various initial conditions, spin rates, inertias, MGM and MTQ sampling times, duty cycles, and quantization effects. The final manuscript will feature numerical investigation of the sensitivity of the control performances, in terms of steady state accuracy and convergence speed, to MGM biases and noises, MTQ biases and noises, CSS errors, and environmental perturbation torques such Gravity Gradient and aerodynamic drag at various altitudes. Furthermore, the switching logic between the various modes will be refined. The remainder of this extended abstract shows a short review of the detumbling and Sun acquisition algorithms as well as preliminary numerical results.

Brief Description of the Detumbling and Sun Acquisition Algorithms

For detumbling purposes, a modified **b**-dot control law, as proposed in [1, 3], is applied. Once the tumbling rate has been dampened sufficiently and a measurement of the Sun vector in the body frame is available, the **b**-dot controller is augmented with a Coarse Sun Pointing algorithm. Once Sun vector measurements, its time derivative and an angular rate estimate (from consecutive vector measurements as shown in [7]) are available, the Fine Sun Pointing control law can be used. This control law is based on a PD controller, which tries to point the Z axis of the satellite to the Sun. The advantage of these modes is that no information on the state of the satellite is required. Only measurements from the MGM and the CSS are needed. Next to that only the MTQ are used as actuators.

Modified b-dot controller

Using only magnetometer measurements and magnetorquers, this spacecraft magnetic dipole is computed as follows

$$\mathbf{M}_{\dot{\mathbf{B}}} = -k_B(\dot{\mathbf{B}} + \boldsymbol{\omega}_d \times \mathbf{B}) \tag{1}$$

where $\mathbf{M}$ is the required dipole, k_B is a positive scalar gain, $\mathbf{B}$ is the measured magnetic field and $\boldsymbol{\omega}_d$ is the desired spin rate around the z-axis (the x and y element are 0). All vectors are projected in the body reference frame and the time derivative of the magnetic field $\dot{\mathbf{B}}$, is computed from successive magnetic field measurements. The resulting torque on the satellite, which is expressed as follows

$$\mathbf{T} = \mathbf{M} \times \mathbf{B} \tag{2}$$

will bring the satellite into a desired spin rate around the z-axis. This control law will be used until the value of $\dot{\mathbf{B}}_z$ remains below a predefined limit for a certain amount of time. Care has to be taken when setting this limit, to not exit this mode prematurely. The other elements of the $\dot{\mathbf{B}}$ vector keep changing, as the satellite will be spinning around the z-axis, close to the desired rate.

Coarse Sun Pointing controller

Following the derumbling mode, once the desired spin rate has been achieved and the Sun vector measurements are available, the Coarse Sun Pointing control mode is entered. This controller lets the z axis precess toward the Sun vector. As the z magnetorquer only produces torques in the XY plane the dot product between the torque $\mathbf{T}$ produced by the z magnetorquer and the Sun vector $\mathbf{S}$ will approach zero when the z-axis is pointing towards the Sun:

$$\begin{aligned} \mathbf{T} \cdot \mathbf{S} &= \mathbf{M} \times \mathbf{B} \cdot \mathbf{S} \\ &= M_z(B_x S_y - B_y S_x) \\ &= 0 \end{aligned} \tag{3}$$

For Eq. (3) to be equal to zero, the (non trivial) solution is to bring $B_x S_y - B_y S_x$ to zero. The commanded magnetic dipole is here

$$\mathbf{M}_{CSP_z} = k_{CSP}(B_x S_y - B_y S_x) \tag{4}$$

where k_{CSP} is a positive scalar gain, which should be carefully selected in order not to interfere with the **b**-dot control and to avoid producing large overshoots. For this purpose, a gain weighter of the form $1 - S_z$ is suggested, which vanishes when the satellite points towards the Sun. The total commanded dipole is as follows

$$\mathbf{M} = \mathbf{M}_{\dot{\mathbf{B}}} + \begin{bmatrix} 0 \\ 0 \\ (1 - S_z)k_{CSP}(B_x S_y - B_y S_x) \end{bmatrix} \tag{5}$$

Notice that the weight $(1 - S_z)$ is positive and smaller than one provided that the Sun vector measurement is unitized. This control law is a modification from the control law suggested in [1, 3]: it features a linear relation rather than an absolute-value based relation.

Fine Sun Pointing controller

Once Coarse Sun Pointing is achieved, the ADCS switches to the Fine Sun Pointing mode. In this mode the time derivative of the Sun vector and the estimated angular rate are needed. The time derivatives are computed from consecutive measurements and the angular rate are computed from consecutive measurements of the magnetic field and the Sun vector, as described in [5], or alternatively using the method in [7] where the magnetic field vector and the Sun vector are assumed inertially constant (which is a good approximation). The control law proposed in [1, 3, 5] is as follows

$$T_z = k_{FSP_s}(\omega_{d_z} - \hat{\omega}_z) \tag{6}$$

where k_{FSP_s} is a positive gain and $\hat{\omega}_z$ is the estimated rotation rate around the z axis. This torque can be converted to a desired dipole with

$$\begin{bmatrix} M_{FSP_x} \\ M_{FSP_y} \end{bmatrix} = \frac{T_z}{B_x^2 + B_y^2} \begin{bmatrix} B_y \\ -B_x \end{bmatrix} \tag{7}$$

Just as in the Coarse Sun Pointing controller the z magnetorquer is used for precession and nutation control. In this controller the x and y component of the Sun vector will be driven to zero. The torque is given by:

$$\mathbf{T} = k_{FSP_p}\hat{\omega}_z \begin{bmatrix} S_x \\ S_y \\ 0 \end{bmatrix} - k_{FSP_d} \begin{bmatrix} \hat{\omega}_z S_x + \dot{S}_y \\ \hat{\omega}_z S_y + \dot{S}_x \\ 0 \end{bmatrix} \tag{8}$$

where k_{FSP_p} and k_{FSP_d} are positive gains. From this equation the magnetic dipole of the z magnetorquer can be calculated as:

$$M_{FSP_z} = \frac{B_x T_y - B_y T_x}{B_x^2 + B_y^2} \tag{9}$$

Equations (7) and (9) provide the control logic for the magnetorquers.

Numerical Simulations - Preliminary Results

In this section some preliminary results of the controllers will be presented. The parameters used in the simulation can be found in Table 1. The simulator takes into account disturbance torques produced by the atmospheric drag, the solar drag, the gravity gradient and residual magnetic dipoles. Noise and biases in the MGM measurements will be modeled and incorporated in the numerical results in the final manuscript. It is assumed that the Sun vector is always available and that the timing between magnetic field measurements and magnetic control is not yet incorporated. In future simulations the above mentioned items will be included, to arrive at a more realistic simulation.

Table 1: Parameters used in the simulations

parameter	value
inclination	75 [deg]
altitude	600 [km]
Prin. Inertia Moments	(0.03699,0.03701,0.00599) [$km.m^2$]
Magnetic Field	IGRF11

Modified b-dot controller

Starting with an initial tumble rate of $\boldsymbol{\omega}_0 = [15, 9, 4]^T$ [deg/s] and a desired spin rate of zero, the simulation runs for 5 orbits. The angular rate is shown in Figure 1. With a desired spin rate of 3 [deg/s] around the z axis, the angular rates develop as shown in Figure 2

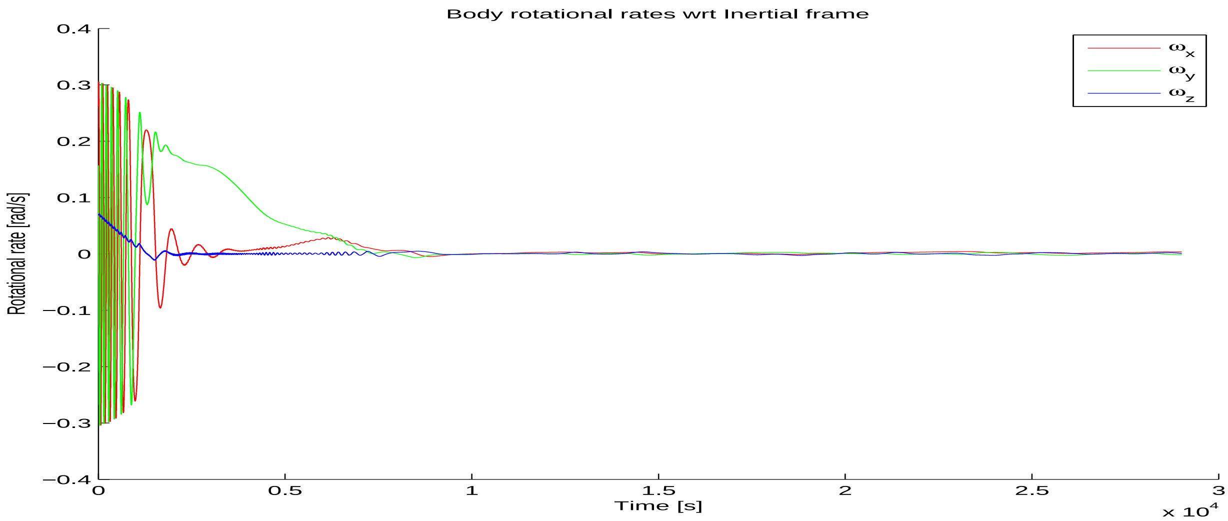

Figure 1: Angular rates as a function of time using the modified **b**-dot controller.

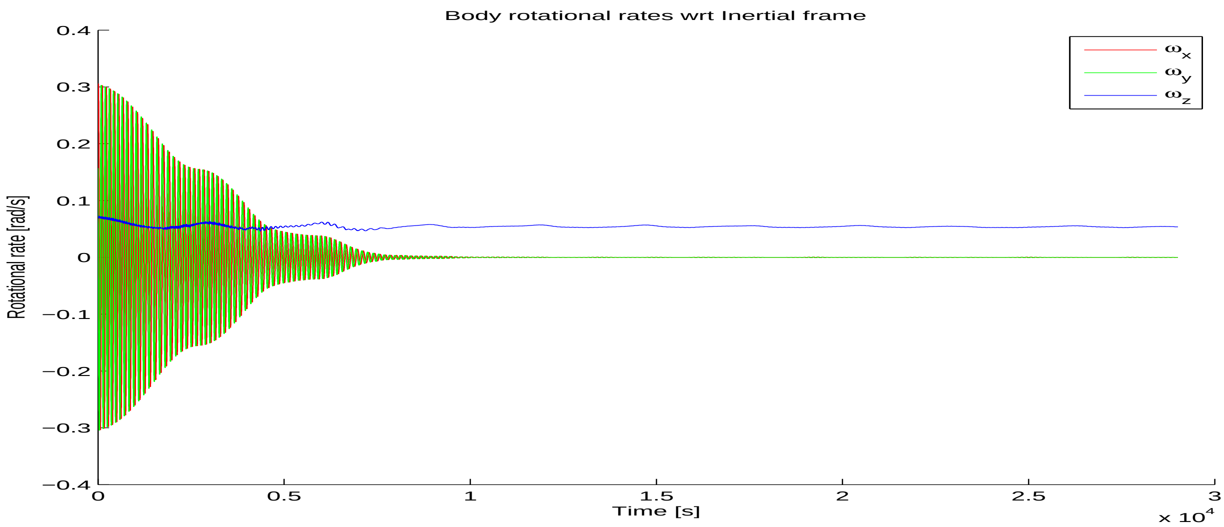

Figure 2: Angular rates as a function of time with desired spin rate of 3 [deg/s] on z axis using the modified **b**-dot controller.

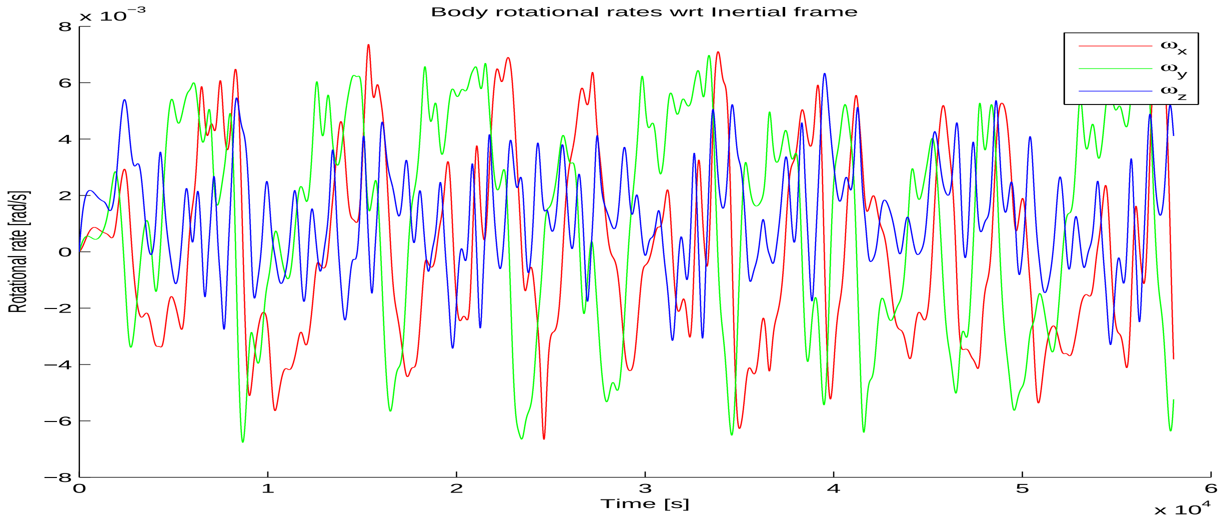

Figure 3: Angular rates as a function of time with desired spin rate of 0 [deg/s] on z axis, using the CSP mode.

Coarse Sun pointing

For the simulations of the Coarse Sun Pointing mode, the satellite starts with the desired spin rate, so the **b**-dot controller does not has to damp the tumbling dynamics.

In Figures 3 and 4 the desired spin rate was 0. It is clear that Sun pointing is not achieved. The controller is here unable to damp the nutation and precession. In the case where the desired spin rate is 3 deg/s, Figures 5 and 6 show that the Sun pointing is reached and kept within an error of 20 degrees within 2 orbits subsequently to the **b**-dot controller.

Fine Sun Pointing

For the Fine Sun Pointing controller the start spin rate is also equal to the desired spin rate. As showed in the Coarse Sun Pointing subsection, Sun pointing can only be achieved when there is some spin available. Below are simulations with a desired spin rate of 3 deg/s around the z-axis. The results are shown in Figures 7 and 8.

References

[1] J. Thienel, R. Bruninga, R. Stevens, C. Ridge, and C. Healy, "The magnetic attitude control system for the parkinson (psat) - a us naval academy designed cubesat," *AIAA*, 2009.

[2] A. C. Stickler and K. T. Alfriend, "Elementary magnetic attitude control system," *AIAA*, 1975.

[3] G. Creamer, "The hessi magnetic attitude control system," *AIAA Guidance Navigation and Control Conference*, Portland, OR, Aug. 1999.

[4] M. L. Psiaki, "Magnetic torquer attitude control via asymptotic periodic linear quadratic regulation," *Journal of Guidance, Control, and Dynamics*, vol. 24, 2000.

[5] C. A. Sedlund, "A simple sun-pointing magnetic controller for satellites in equatorial orbits," *IEEE Aerospace Conference*, Big Sky, MT, March 2009.

[6] D. Verbin and S. Mualem, "Minimal configuration attitude control for nano satellite," *Proceedings of the Israel Annual Conference on Aeronautical Sciences*, Tel-Aviv, Israel, Feb. 2011.

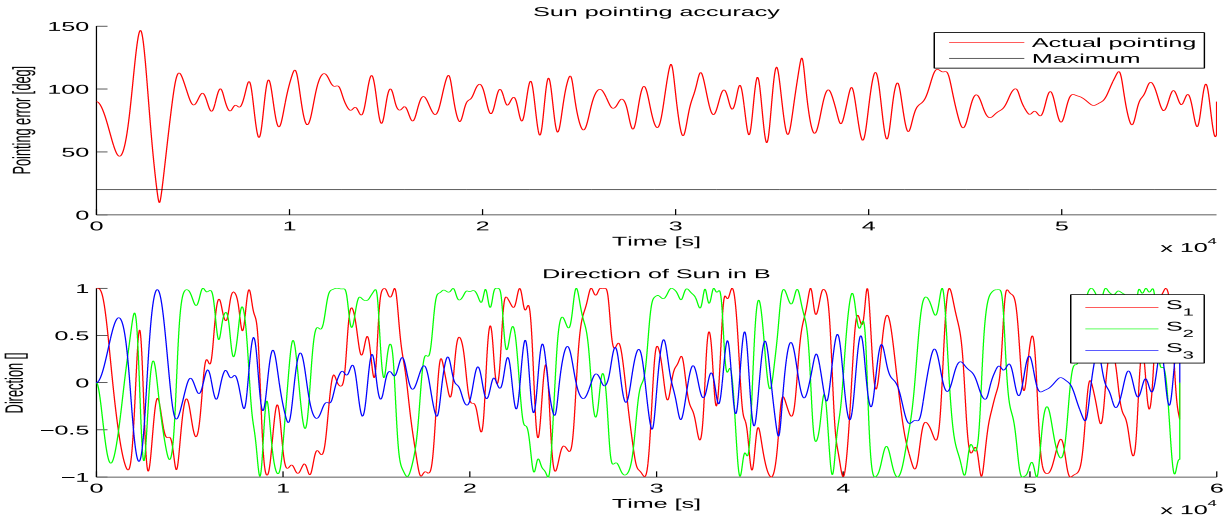

Figure 4: Sun vector pointing as a function of time with desired spin rate of 0 [deg/s] on z axis, using the CSP mode.

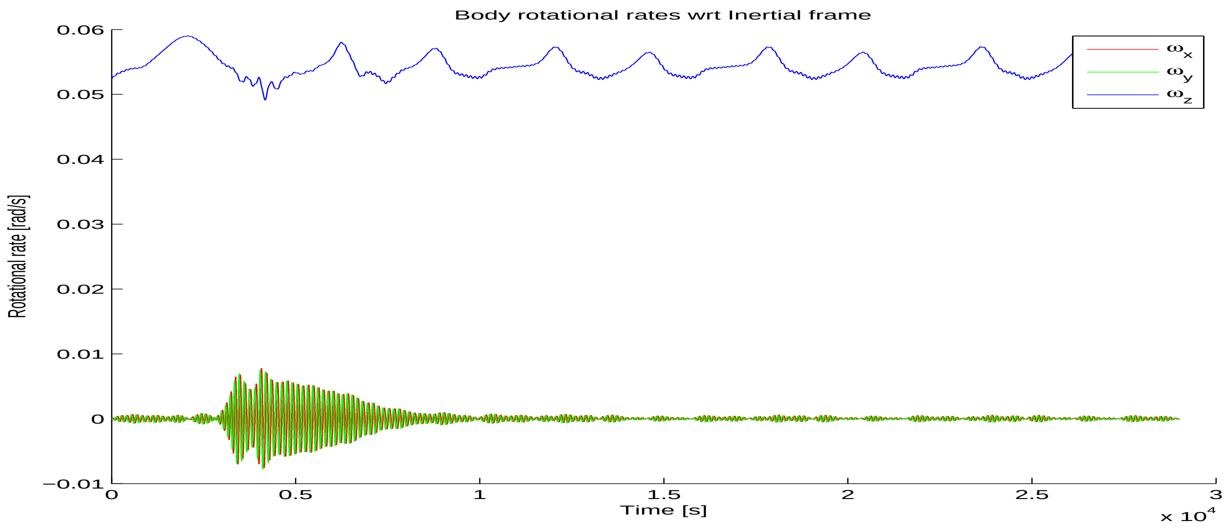

Figure 5: Angular rates as a function of time with desired spin rate of 3 [deg/s] on z axis, using the CSP mode.

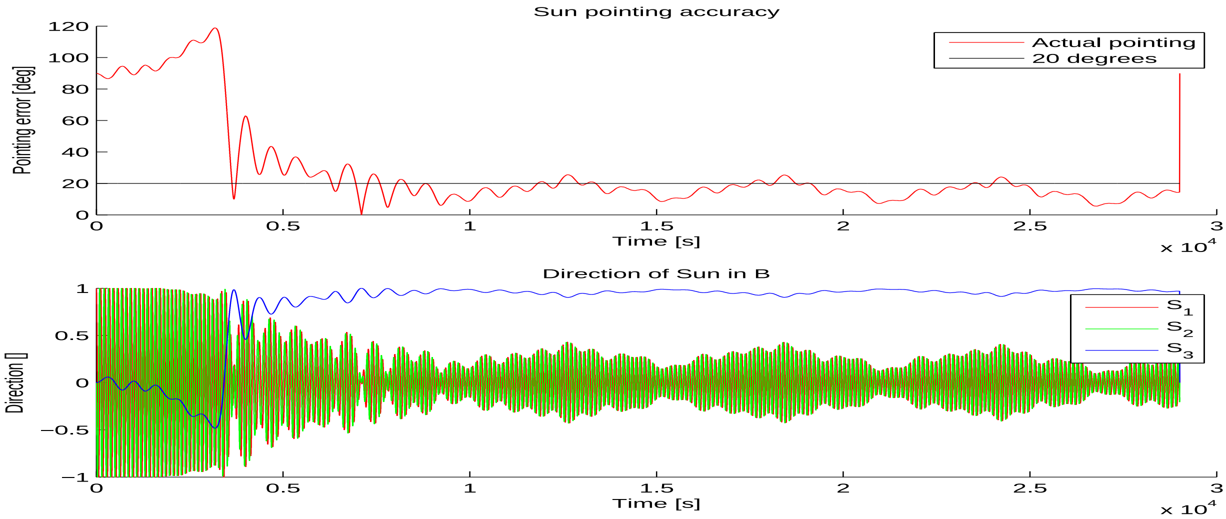

Figure 6: Sun vector pointing as a function of time with desired spin rate of 3 [deg/s] on z axis, using the CSP mode.

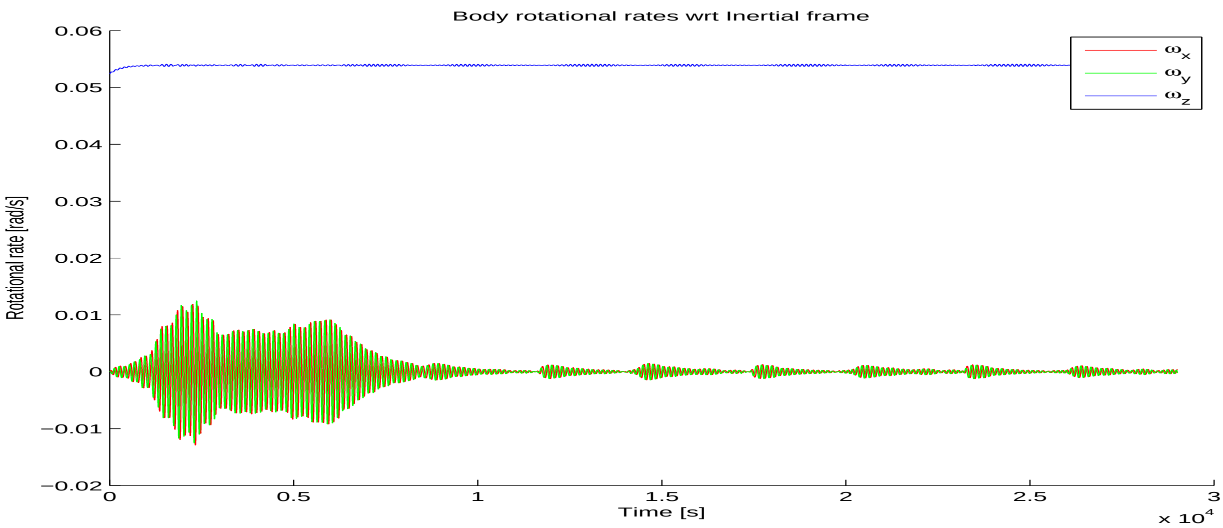

Figure 7: Angular rates as a function of time with desired spin rate of 3 [deg/s] on z axis, using the FSP mode.

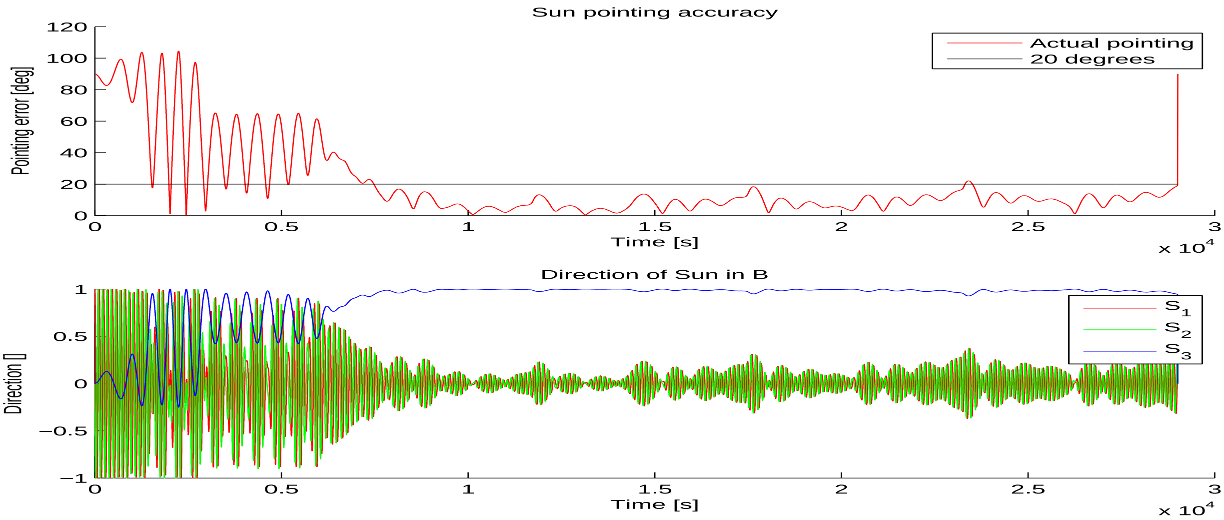

Figure 8: Sun vector pointing as a function of time with desired spin rate of 3 [deg/s] on z axis, using the FSP mode.

[7] R. Azor, I. Y. Bar-Itzhack, and R. R. Harman, "Satellite angular rate estimation from vector measurements," *AIAA - Journal of Guidance, Control and Dynamics*, 1998.